Modeling Surface-Roughness-Induced Scattering in Non-Planar Silicon Nanostructures

Z. Stanojević, H. Kosina
TU Wien, Institute for Microelectronics, Gußhausstraße 27-29/E360, 1040 Wien, Austria
Tel. +43-1-58801-36016, FAX: +43-1-58801-36099, (stanojevic,kosina)@iue.tuwien.ac.at

I. Introduction

We extend the surface roughness scattering formalism for planar structures to non-planar ones. The planar-structure formalism based on theory by Prange and Nee [1] has been widely used for calculating the conductivity of inversion layers and thin films [2]. An extension to cylindrical nanowires has been developed by Jin et al. [3]; their model assumes isotropic band structure in the channel matrial and assigns radial and angular quantum numbers to each state thus facilitating the evaluation of the surface roughness matrix elements.

We derive matrix elements for open and closed surfaces of arbitrary shape taking anisotropy of the band structure fully into account. This model is applied to different device cross-sections such as a FinFET or a nanowire.

II. Method

To evaluate the ensemble average of the surface roughness scattering rate for a one-dimensional carrier gas

$$\langle S_{n,n'}(k,k')\rangle = \frac{\hbar}{2\pi}\langle|H_{n,n';k,k'}|^2\rangle\delta(E(k)-E(k')) \qquad (1)$$

we write the square of the unscreened matrix element as

$$\langle|H_{n,n';k,k'}|^2\rangle = \frac{1}{L^2}\iint_{\mathscr{C}} \mathrm{d}s\mathrm{d}s' \iint_0^L \mathrm{d}z\mathrm{d}z'$$
$$f_{n,n';k,k'}(s) f^*_{n,n';k,k'}(s') e^{i(k-k')(z-z')}\langle\Delta(\mathbf{r})\Delta(\mathbf{r}')\rangle, \qquad (2)$$

where $\Delta(\mathbf{r})$ is the random fluctuation of the surface of which only the autocorrelation $c(\mathbf{r}) = \langle\Delta(\mathbf{r}')\Delta(\mathbf{r}'+\mathbf{r})\rangle$ and its 2D Fourier transform $C(\mathbf{q})$ are known; no assumptions are made about the nature of $c(\mathbf{r})$ or $C(\mathbf{q})$ and the model works with any kind of autocorrelation. The intersection of the rough surface and the cross-section plane forms the curve $\mathscr{C}$; s denotes the path coordinate along the curve and z the axial coordinate (see Fig. 1). The surface field factors $f_{n,n';k,k'}(s)$ are defined as $\psi^*_{n,k}\psi_{n',k'}\Delta V$, with the cross-section wave functions $\psi_{n,k}$ and the potential step ΔV on the surface.

Expression (2) can be simplified to

$$\langle|H_{n,n';k,k'}|^2\rangle = \frac{1}{2\pi L}\int_{-\infty}^{\infty} |F_{n,n';k,k'}(q_\perp)|^2 C(\hat{q})\mathrm{d}q_\perp, \qquad (3)$$

where the integration is performed over $q_\perp$, the roughness "wavenumber" in the cross-section plane. $F_{n,n';k,k'}(q_\perp)$ are Fourier transforms of the form factors $f_{n,n';k,k'}$ and $\hat{q} = \sqrt{q_\perp^2 + (k-k')^2}$ assuming isotropic roughness autocorrelation. The integral (3) accurately captures the roughness-induced momentum transfer between the confined states.

III. Results

We demonstrate the capabilities of the developed model using two example devices: a gated silicon nanowire and a bulk silicon FinFET. The nanowire is cylindrical, measures $10\,\mathrm{nm}$ in diameter and is covered by $2\,\mathrm{nm}$ of $\mathrm{SiO_2}$. The FinFET is of bulk type; the fin is of trapezoidal shape, $20\,\mathrm{nm}$ high, $12\,\mathrm{nm}$ wide at its base and $6\,\mathrm{nm}$ at its top. The channel of both devices has $\langle 100\rangle$ orientation.

First, a self-consistent Schrödinger-Poisson solution is obtained for each device and multliple gate biases, as seen in Fig. 2. Subsequently, scattering rates and low-field channel conductivities are computed from the wavefunctions and subbands calculated in the previous step using the Kubo-Greenwood formula [4]. This procedure allows us to examine the gate bias dependence of both the scattering rates and conductivities. The roughness is assumed to be of exponential autocorrelation [5] with a RMS-amplitude of $0.5\,\mathrm{nm}$ and a correlation length of $2\,\mathrm{nm}$.

Fig. 3 and 4 show the surface-roughness-limited (SR) and acoustic-phonon-limited (ADP) channel conductivities in different conduction band valleys for the nanowire and FinFET device. The ADP-limited conductivity increases almost linearly with gate bias. In contrast, the SR-limited conductivity begins to saturate at low inversion charge; for higher gate voltages some valleys even exhibit a negative differential transconductance.

Fig. 5 and 6 show the ADP and SR scattering rates in the lowest subband of the nanowire and FinFET. Compared to ADP, SR is anisotropic and has a higher mode-selectiveness.

IV. Conclusion

We developed a new generic method for evaluating the surface-roughness-induced scattering rate in non-planar semiconductor structures, which is a consistent extension of previous work on planar inversion layers and thin films. Example calculations were conducted to test the method.

Acknowledgment

This work has been supported by the Austrian Science fund through contracts F2509 and I841-N16.

References

[1] R. E. Prange *et al.*, Phys. Rev. **168**, 779 (1968).
[2] D. Esseni, IEEE T. Electron. Dev. **51**, 394 (2004).
[3] S. Jin *et al.*, J. Appl. Phys. **102**, 083715 (2007).
[4] D. A. Greenwood, Proc. Phys. Soc. **71**, 585 (1958).
[5] S. M. Goodnick *et al.*, Phys. Rev. B **32**, 8171 (1985).

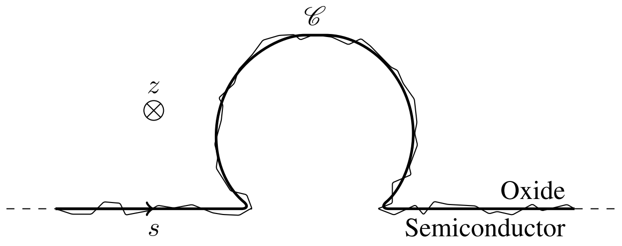

Fig. 1. Schematic view of the rough oxide-semiconductor interface; the ideal structure is translationally invariant along the z axis. The intersection between the cross-section plane and the interface forms the curve $\mathscr{C}$. A path coordinate s is defined along $\mathscr{C}$.

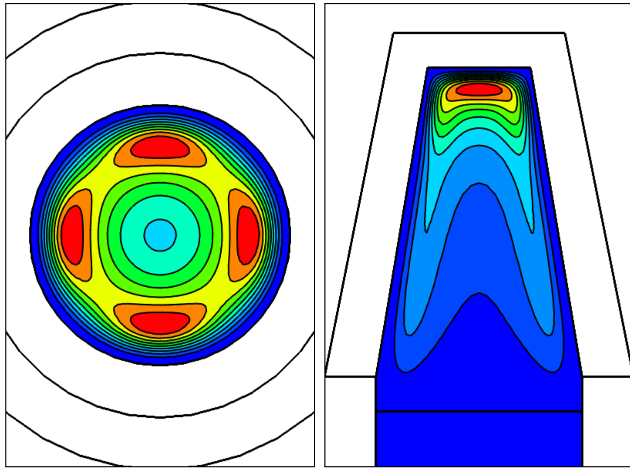

Fig. 2. Electron concentration in a gated nanowire (left) and FinFET (right); the effect of band anisotropy is clearly visible in the nanowire.

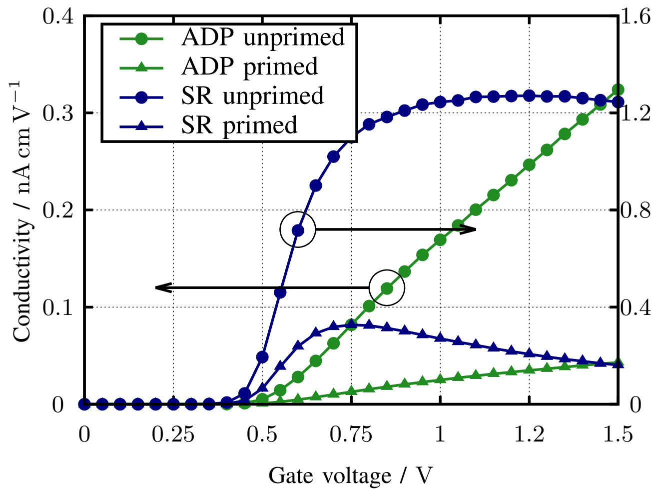

Fig. 3. Conductivities in the gated nanowire for the unprimed and primed valleys; the ADP-limited conductivity increases almost linearly with the gate voltage, i.e. the conductivity curve follows the inversion charge. The SR-limited curve begins to saturate already at low gate voltages due to the carriers being pressed againts the rough surface. For high gate voltages a negative differential transconductance is noticeable in the SR-limited curve.

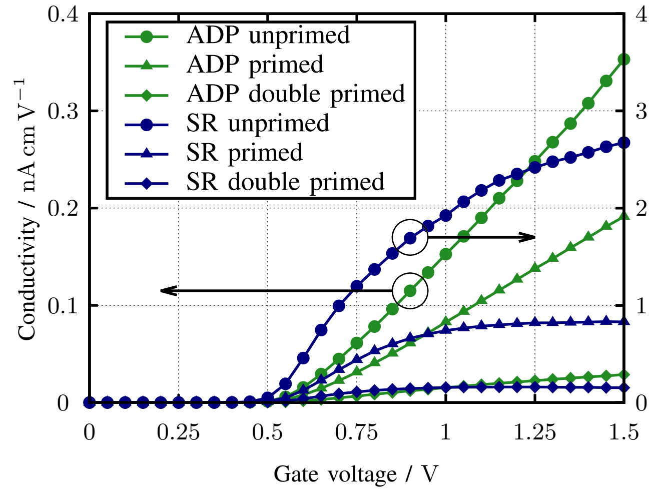

Fig. 4. Conductivities in the FinFET; here, each of the three valleys behaves differently since no rotational symmetry is present. Same effects as in Fig. 3 can be observed.

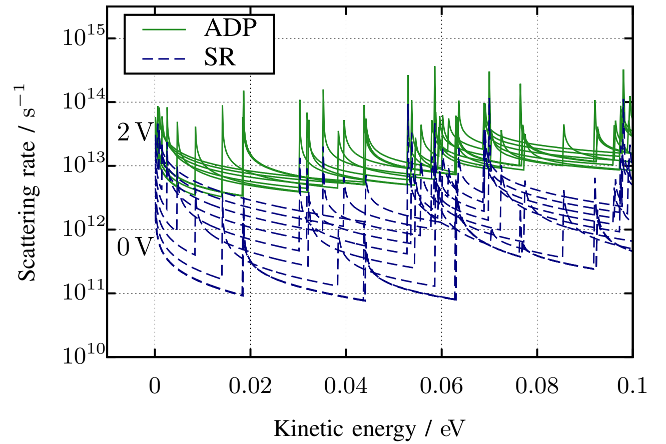

Fig. 5. Momentum scattering rates for the lowest subband in the gated nanowire at different gate biases ranging from 0 to 2 V; SR scattering increases strongly with gate bias, varying over more than one decade. The ADP scattering rate increases only slightly with gate bias

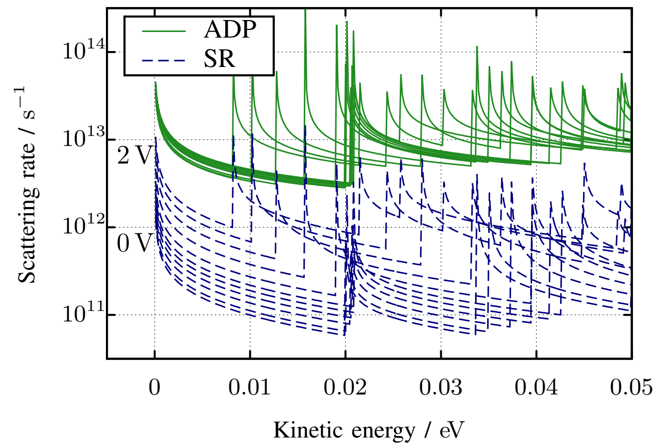

Fig. 6. Momentum scattering rates for the lowest subband in the FinFET at different gate biases; similar behavior of the rates as in Fig. 5 can be observed.